Electronic Supplementary Material (ESI) for Environmental Science: Nano.

Support Information for

SERS-based Detection of an Organochlorine Pesticide Through Surface Plasmon-Induced C-C Coupling

-

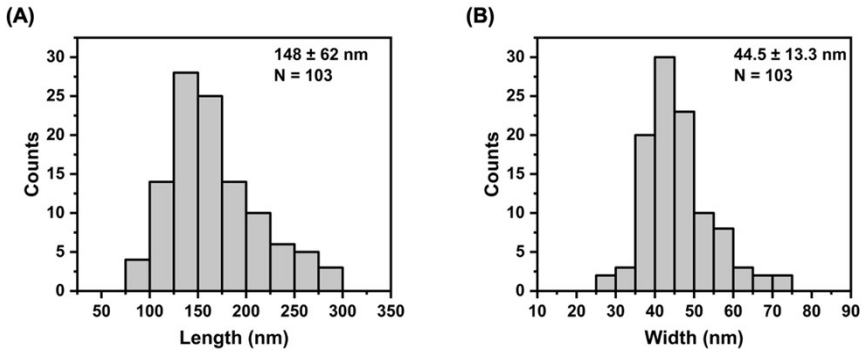

Figure S1. Particle size distributions for AgNRs **(A)** length and **(B)** width.

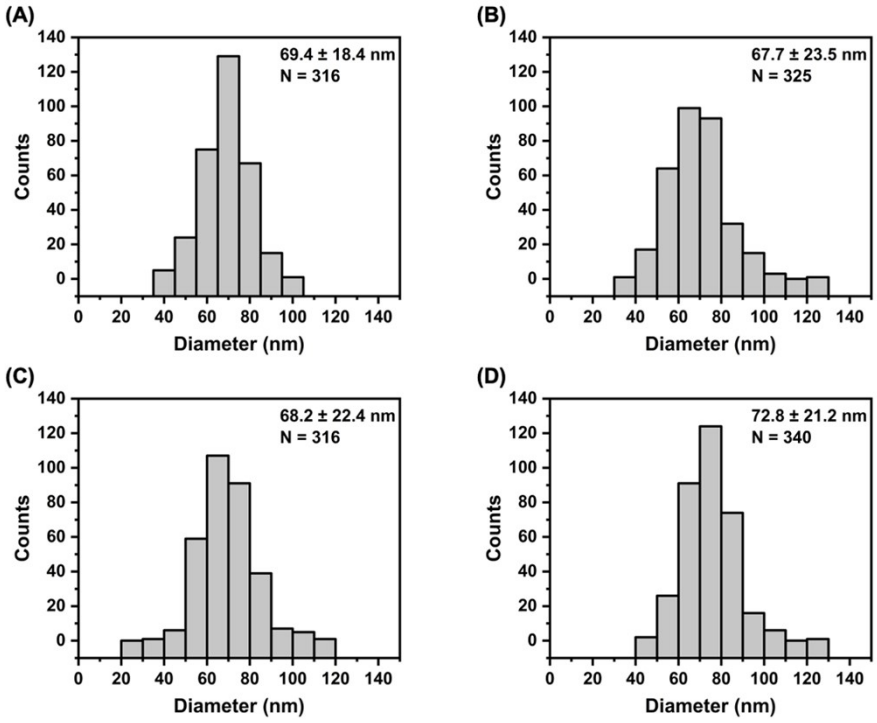

Figure S2. Particle size distributions for **(A)** AgNPs, **(B)** $AgPd_{2.5\ mol\%}$NPs, **(C)** $AgPd_{5.0\ mol\%}$NPs and **(D)** $AgPd_{10\ mol\%}$NPs.

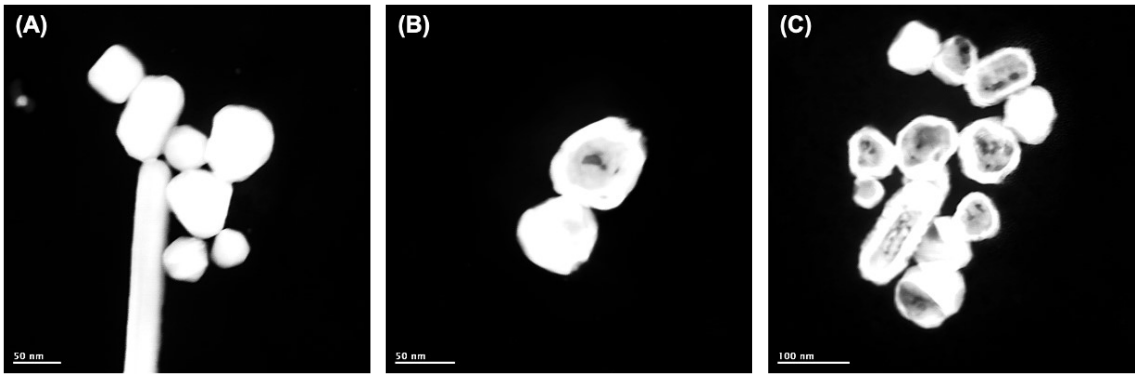

Figure S3. Representative HAADF-STEM for **(A)** $AgPd_{2.5\ mol\%}$NPs, **(B)** $AgPd_{5.0\ mol\%}$NPs, and **(C)** $AgPd_{10\ mol\%}$NPs.

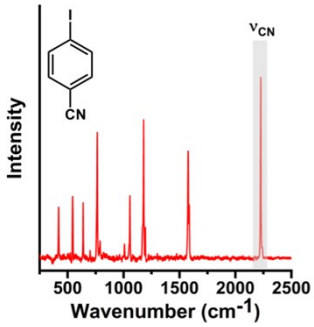

Figure S4. Ordinary Raman spectrum of 4-IBN powder.

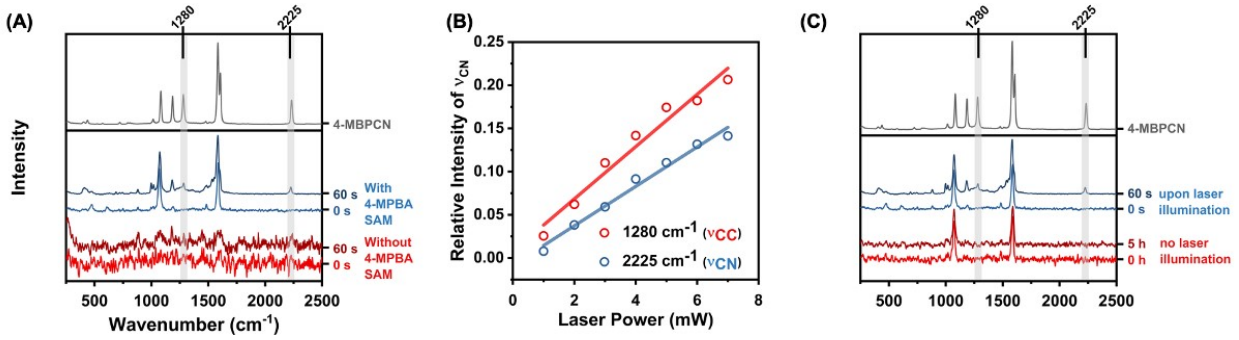

Figure S5. (A) SERS spectra of bare $AgPd_{5.0\ mol\%}$NPs (red; without 4-MPBA SAM) and 4-MPBA-functionalized $AgPd_{5.0\ mol\%}$NPs (blue; with 4-MPBA SAM) immersed in 5mM 4-IBN solution before (0 s) and after (60 s) 633 nm laser illumination. Power: 1.0 mW. The SERS spectrum of 4-MBPCN on $AgPd_{5.0\ mol\%}$NPs is also shown at the top for reference. **(B)** Evolution of the relative intensities of the bands at 1285 and 2225 cm^{-1} (assigned to 4-MBPCN) to that at 1072 cm^{-1} (combined contribution of 4-MBPCN and 4-MPBA) as a function of incoming laser power, determined from the integrated intensity of ν_{CC} and ν_{CN} in Figure 2E. **(C)** SERS spectra of 4-MPBA-functionalized $AgPd_{5.0\ mol\%}$NPs immersed in 5 mM 4-IBN solution kept in the dark (red, no laser illumination, at 0 h and 5 h) and kept under 633 nm laser irradiation (blue, upon laser illumination, at 0 s and 60 s). Power: 1.0 mW. The SERS spectrum of 4-MBPCN on $AgPd_{5.0\ mol\%}$NPs is also shown at the top for reference.

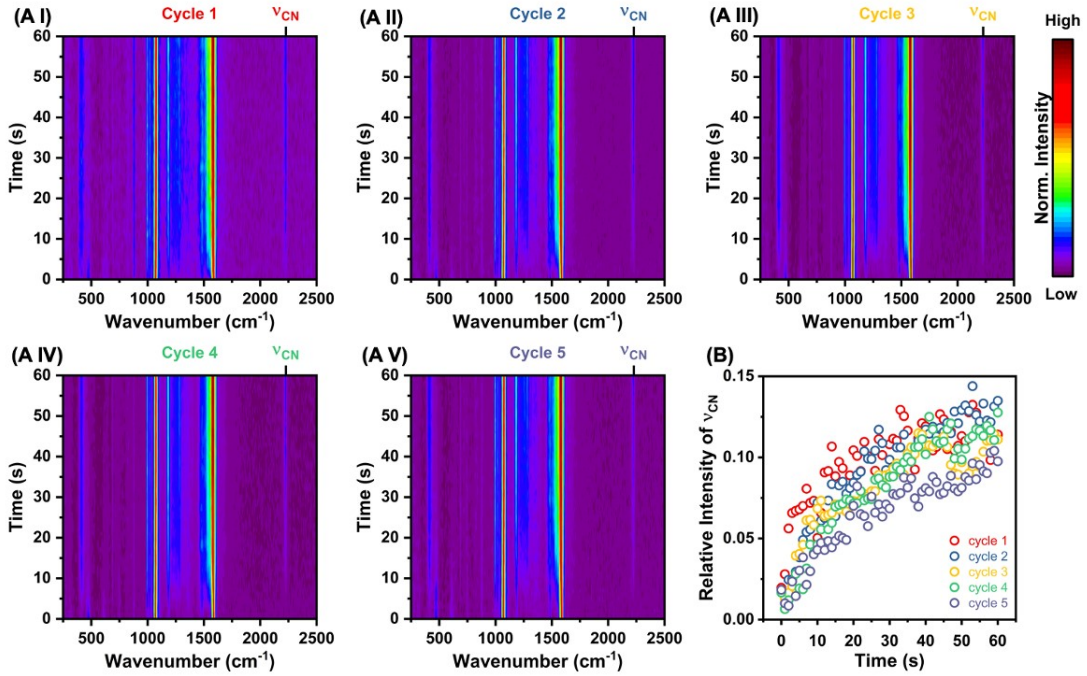

Figure S6. (A) Time-dependent in situ SERS spectra of the Suzuki-Miyaura coupling for 4-MPBA SAM on $AgPd_{5.0\ mol\%}$NPs in 5 mM 4-IBN solution upon exposure to 633 nm laser illumination over **(AI-AV)** 5 cycles of reactions. Power: 1.0 mW. **(B)** Temporal evolution of the relative intensity of the band at 2225 cm^{-1} (assigned to 4-MBPCN) to that at 1072 cm^{-1} (combined contribution of 4-MBPCN and 4-MPBA) over 5 cycles of reactions.

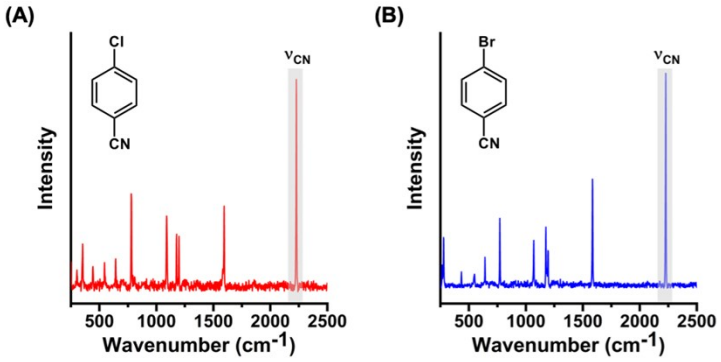

Figure S7. Ordinary Raman spectrum of **(A)** 4-CBN and **(B)** 4-BBN powder.

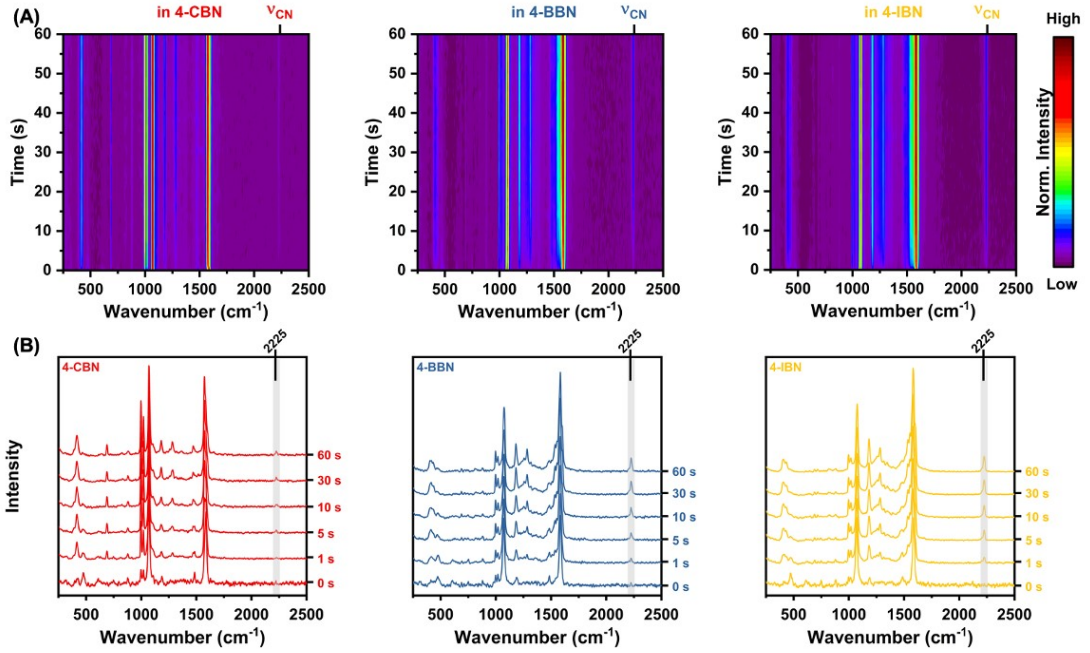

Figure S8. (A) Time-dependent in situ SERS spectra of the Suzuki-Miyaura coupling for 4-MPBA SAM on $AgPd_{5.0\ mol\%}$NPs in 10 mM 4-CBN, 4-BBN and 4-IBN solution upon exposure to 633 nm laser illumination. Power: 1.0 mW. **(B)** SERS spectra recorded at selected time intervals during Suzuki-Miyaura reaction.

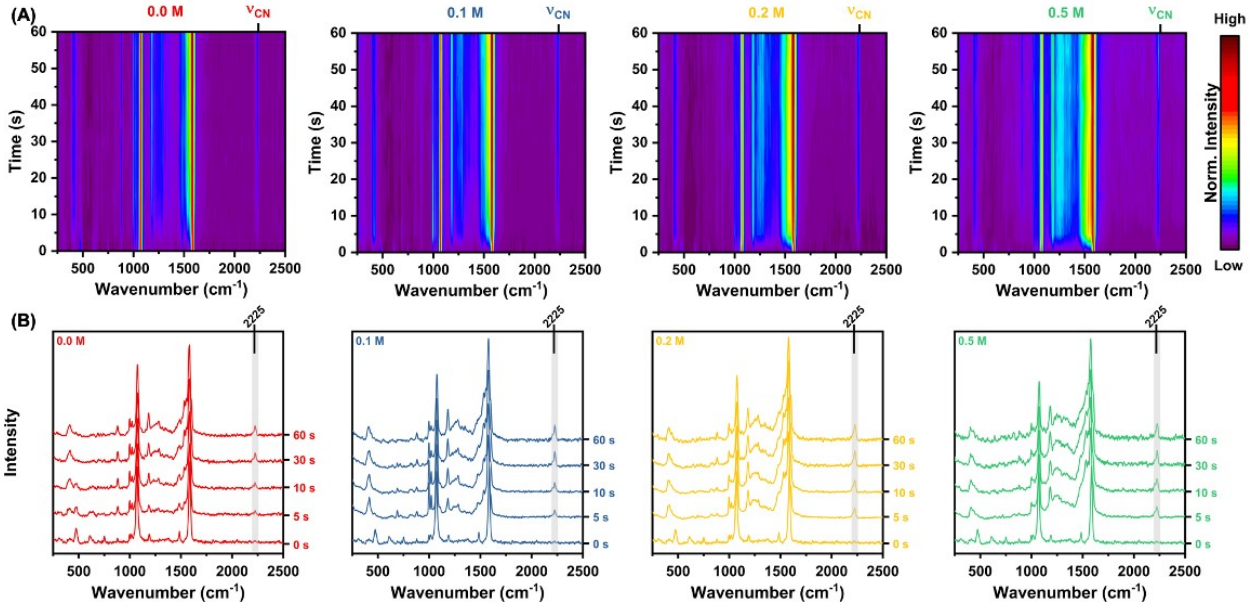

Figure S9. (A) Time-dependent in situ SERS spectra of the Suzuki-Miyaura coupling for 4-MPBA SAM on $AgPd_{5.0\ mol\%}$NPs in 5 mM 4-IBN alkaline solution upon exposure to 633 nm laser illumination after addition of 0.0; 0.1; 0.2 and 0.5 M NaOH. Power: 1.0 mW. **(B)** SERS spectra recorded at selected time intervals during Suzuki-Miyaura reaction.

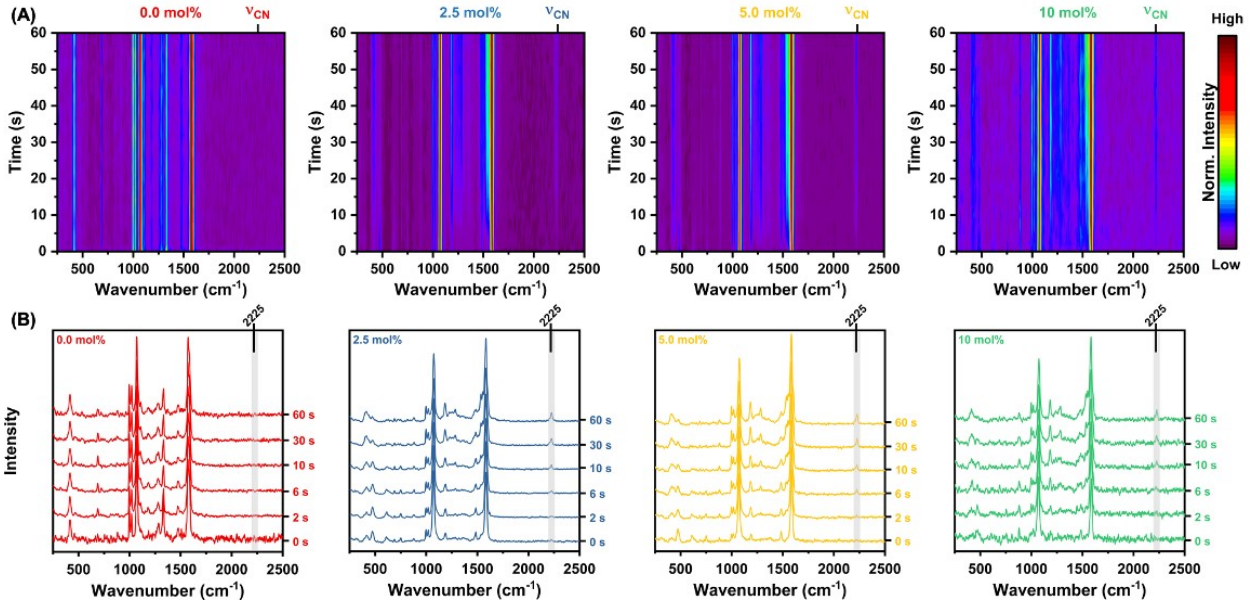

Figure S10. (A) Time-dependent in situ SERS spectra of the Suzuki-Miyaura coupling for 4-MPBA SAM on $AgPd_{x\ mol\%}NPs$ (x = 0.0; 2.5; 5.0 and 10 mol%) in 5 mM 4-IBN solution upon exposure to 633 nm laser illumination. Power: 1.0 mW. **(B)** SERS spectra recorded at selected time intervals during Suzuki-Miyaura reaction.

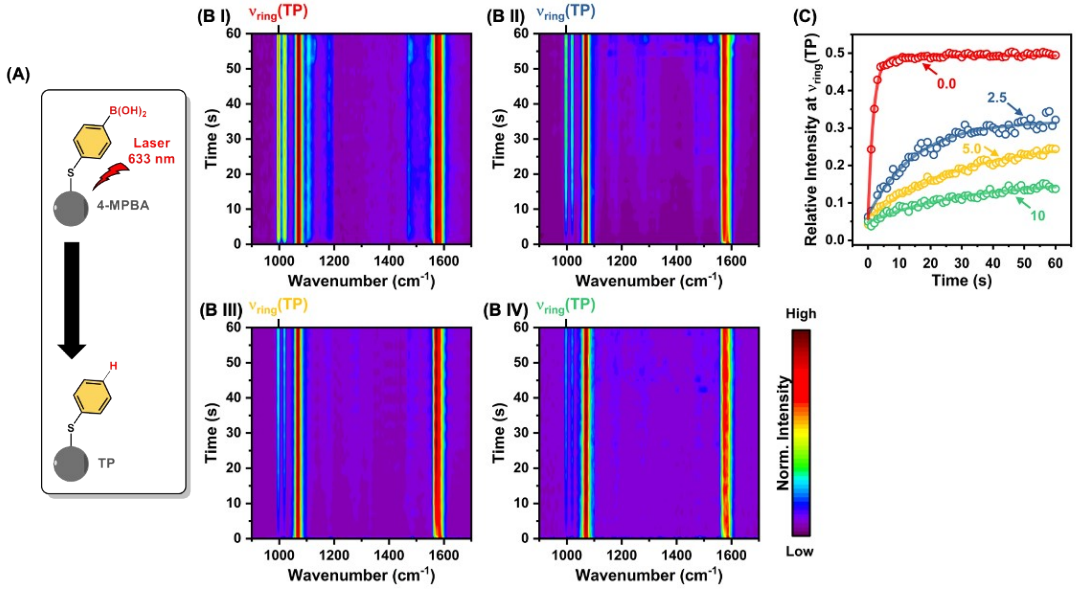

Figure S11. (A) Schematic illustration of SP-induced protodeboronation of 4-MPBA to TP on $AgPd_{x\ mol\%}NPs$ surfaces. **(B)** Time-dependent in situ SERS spectra of the protodeboronation of 4-MPBA SAM on **(B I)** AgNPs, **(B II)** $AgPd_{2.5\ mol\%}NPs$, **(B III)** $AgPd_{5.0\ mol\%}NPs$, and **(B IV)** $AgPd_{10\ mol\%}NPs$ under air upon exposure to 633 nm laser illumination. Power: 1.0 mW. **(C)** Temporal evolution of the relative intensity of the band 999 cm^{-1} (assigned to TP) to that at 1072 cm^{-1} (combined contribution of TP and 4-MPBA) as a function of the Pd loading on $AgPd_{x\ mol\%}NPs$.

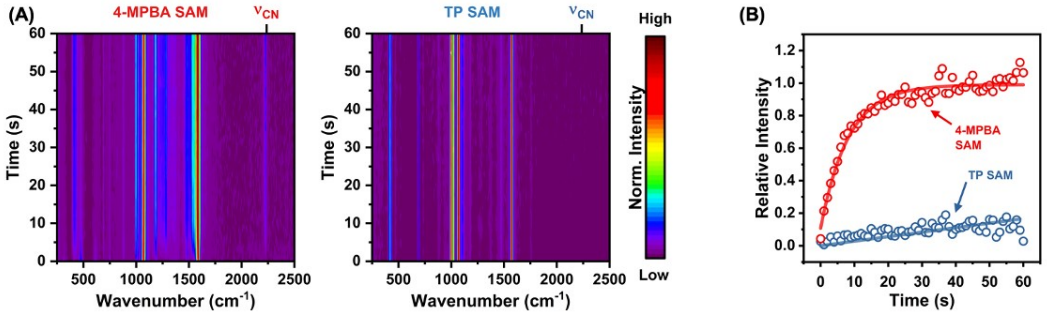

Figure S12. (A) Time-dependent in situ SERS spectra of the Suzuki-Miyaura coupling for 4-MPBA SAM (left, red) and TP SAM (right, blue) on $AgPd_{5.0\ mol\%}$ NPs in 5 mM 4-IBN solution upon exposure to 633 nm laser illumination. Power: 1.0 mW. **(B)** Temporal evolution of the relative intensity of the band at 2225 cm^{-1} (assigned to 4-MBPCN) to that at 1072 cm^{-1} (combined contribution of 4-MBPCN and 4-MPBA) for 4-MPBA SAM (red) and TP SAM (blue) on $AgPd_{5.0\ mol\%}$ NPs.

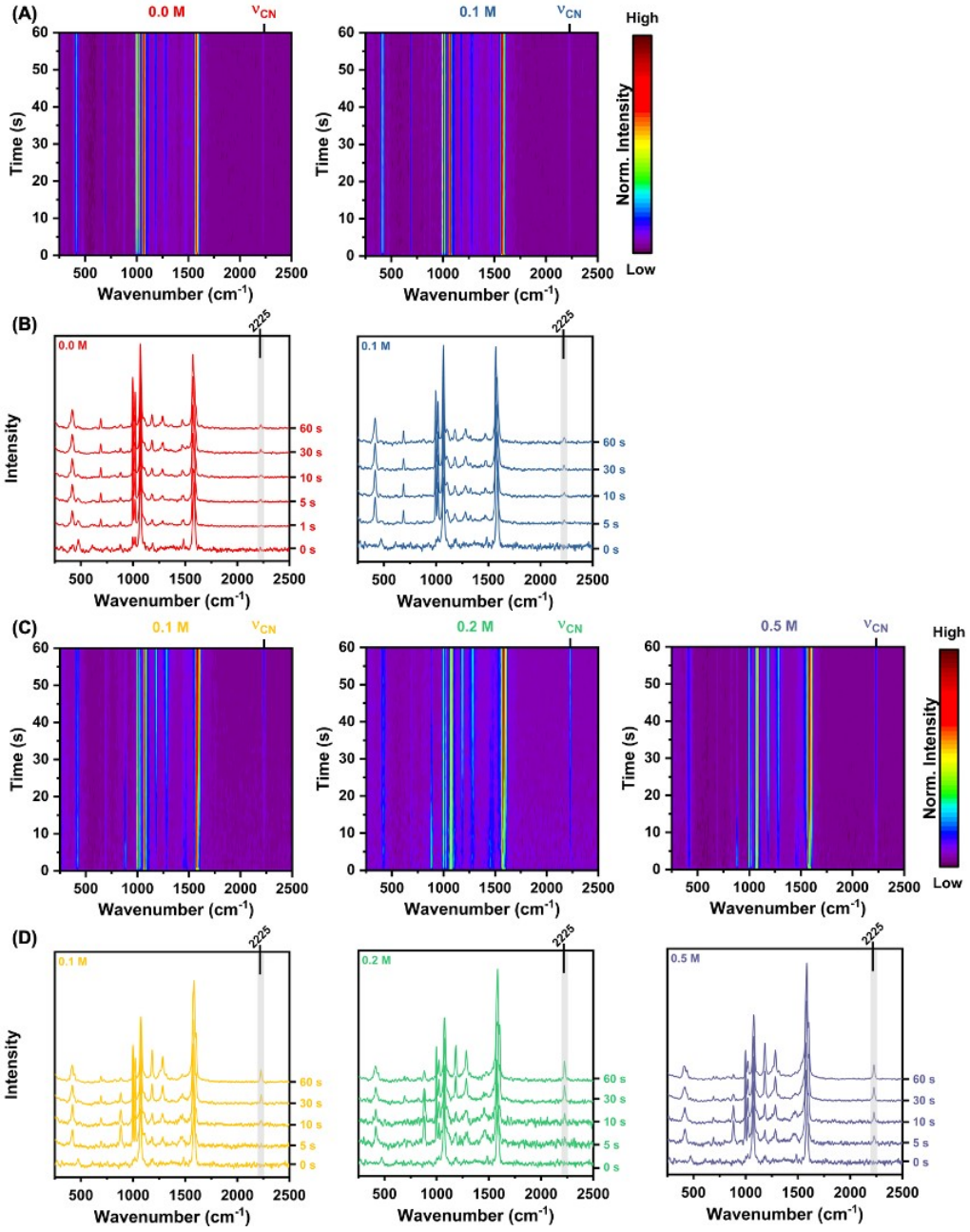

Figure S13. (A) Time-dependent in situ SERS spectra of the Suzuki-Miyaura coupling for 4-MPBA SAM on $AgPd_{5.0\ mol\%}$NPs in 5 mM 4-CBN solution upon exposure to 633 nm laser illumination after addition of 0.0 and 0.1 M NaOH. Power: 1.0 mW. **(B)** SERS spectra recorded at selected time intervals during Suzuki-Miyaura reaction at incoming laser power equal to 1.0 mW. **(C)** Time-dependent in situ SERS spectra of the Suzuki-Miyaura coupling for 4-MPBA SAM on $AgPd_{5.0\ mol\%}$NPs in 5 mM 4-CBN solution upon exposure to 633 nm laser illumination after addition of 0.1; 0.2 and 0.5 M NaOH. Power: 5.0 mW. **(D)** SERS spectra recorded at selected time intervals during Suzuki-Miyaura reaction at incoming laser power equal to 5.0 mW.

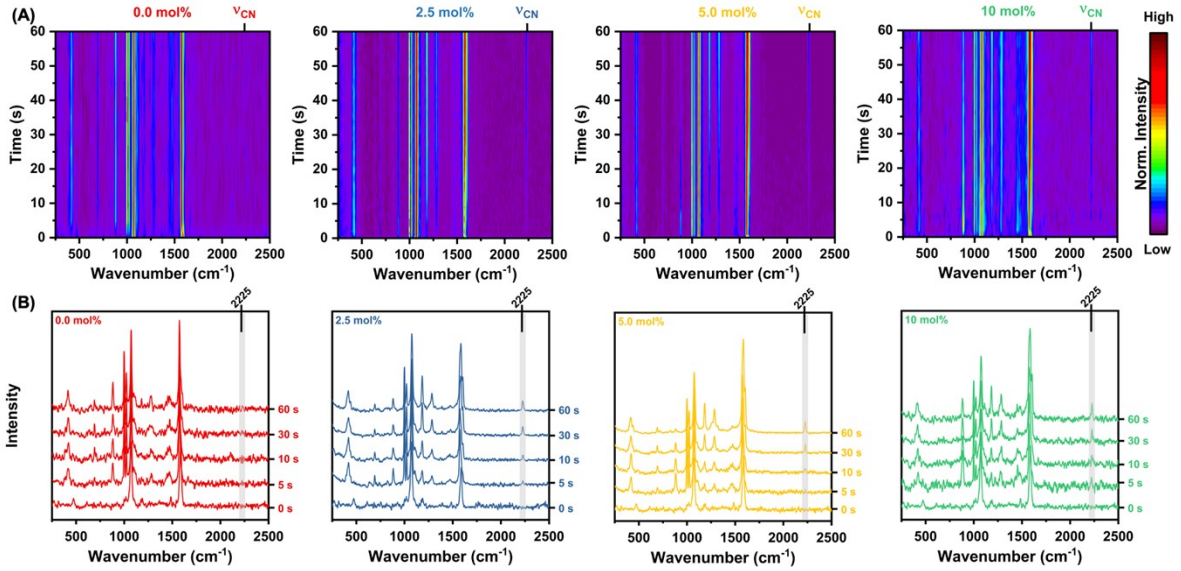

Figure S14. (A) Time-dependent in situ SERS spectra of the Suzuki-Miyaura coupling for 4-MPBA SAM on $AgPd_{x\ mol\%}$NPs (x = 0.0; 2.5; 5.0 and 10 mol%) in 5 mM 4-CBN alkaline solution (0.1 M NaOH) upon exposure to 633 nm laser illumination. Power: 5.0 mW. **(B)** SERS spectra recorded at selected time intervals during Suzuki-Miyaura reaction.

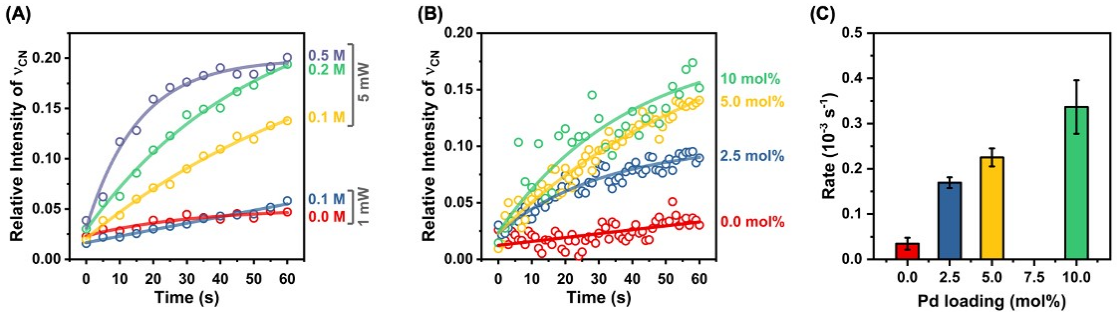

Figure S15. Temporal evolution of the relative intensity of the band 2225 cm^{-1} (feature peak of 4-MBPCN) to that at 1072 cm^{-1} (contributed from both 4-MBPCN and 4-MPBA) as a function of **(A)** the NaOH concentration in a 5 mM 4-CBN alkaline solution at incoming 1.0 and 5.0 mW incoming laser power; and **(B)** the Pd loading on 4-MPBA-functionalized $AgPd_{x\ mol\%}$NPs in 5 mM 4-CBN alkaline solution (0.1 M NaOH). Power: 5.0 mW. **(C)** SP-induced Suzuki-Miyaura reaction rate as a function of the Pd loading on $AgPd_{x\ mol\%}$NPs, determined from the slope of the initial linear portion of SERS intensity-time profiles in Figure S15B.

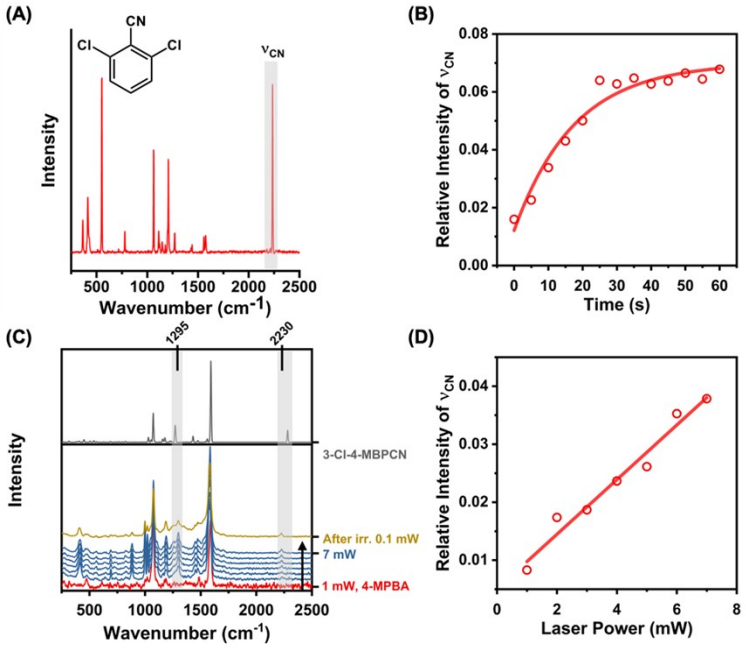

Figure S16. (A) Ordinary Raman spectrum of dichlobenil powder. **(B)** Temporal evolution of the relative intensity of the band at 2225 cm^{-1} (assigned to 4-MBPCN) to that at 1072 cm^{-1} (combined contribution of 4-MBPCN and 4-MPBA) for 4-MPBA SAM on $AgPd_{5.0\ mol\%}$ NPs in 5.0 mM dichlobenil alkaline solution (0.1 M NaOH). **(C)** Laser power-dependent SERS spectra of 4-MPBA SAM on $AgPd_{5.0\ mol\%}$ NPs in 5.0 mM dichlobenil alkaline solution (0.1 M NaOH). Integration time: 1.0 s. The intensity is normalized by the 1072 cm^{-1} Raman peak. **(D)** Evolution of the relative intensity of the band at 2225 cm^{-1} (assigned to 4-MBPCN) to that at 1072 cm^{-1} (combined contribution of 4-MBPCN and 4-MPBA) as a function of incoming laser power, determined from the integrated intensity of ν_{CN} in Figure S16B.